We are IntechOpen, the world's leading publisher of Open Access books Built by scientists, for scientists

6,900
Open access books available

185,000
International authors and editors

200M
Downloads

Our authors are among the

154
Countries delivered to

TOP 1%
most cited scientists

12.2%
Contributors from top 500 universities



WEB OF SCIENCE™

Selection of our books indexed in the Book Citation Index in Web of Science™ Core Collection (BKCI)

Interested in publishing with us?
Contact book.department@intechopen.com

Numbers displayed above are based on latest data collected.
For more information visit www.intechopen.com



Chapter

Numerical Investigations of Electromagnetic Oscillations and Turbulences in Hall Thrusters Using Two Fluid Approach

Sukhmander Singh, Bhavna Vidhani and Ashish Tyagi

Abstract

The first part of the contributed chapter discuss the overview of electric propulsion technology and its requirement in different space missions. The technical terms specific impulse and thrust are explained with their relation to exhaust velocity. The shortcoming of the Hall thrusters and its erosion problems of the channel walls are also conveyed. The second part of the chapter discuss the various waves and electromagnetic instabilities propagating in a Hall thruster magnetized plasma. The dispersion relation for the azimuthal growing waves is derived analytically with the help of magnetohydrodynamics theory. It is depicted that the growth rate of the instability increases with magnetic field, electron drift velocity and collisional frequency, whereas it is decreases with the initial drift of the ions.

Keywords: electric propulsion, Hall thruster, dispersion, impulse, exhaust velocity, growth rate

1. Introduction

In the past few years, electric propulsion has received widespread attention as an alternative to chemical propulsion for spacecraft. A chemical thruster is capable of producing high thrust, but it provides a relatively low specific impulse. This limitation of chemical thrusters opens up discussion of the use of electric thrusters, which provide much higher specific impulses. A high specific impulse allows the spacecraft to reach the same speed with lower propellant consumption than chemical ones or travel faster with the same propellant mass [1–10]. In addition, the use of a high specific impulse, electric thruster permits a significant reduction in propellant mass on spacecraft, which helps reduce launching cost, extending mission lifetime or increase the payload mass on the spacecraft [2]. Therefore, the benefits that electric thrusters provide make them the best choice for in-space propulsion of spacecraft.

To date, several different types of electric propulsion thrusters have been developed, of which Hall thrusters are the most reliable and widely used. Hall thrusters are simple in design, consisting of an annular discharge channel, an anode, a cathode and a radial magnetic field across the channel [1]. A propellant, usually Xenon, is injected to channel through the hollow anode and a high potential difference is

IntechOpen

applied between the anode and cathode. The electrons emitted from the cathode and start moving towards the anode due to the potential difference. As they enter the discharge channel, they get trapped in the radial magnetic field generated by electromagnetic coils (or permanent magnets) and start drifting in the azimuthal direction (E x B). Due to this trapping, the residence time of electrons in the discharge channel increases and they move very slowly towards the anode. Electrons, then collide with neutral propellant atoms entering the discharge channel and ionize them. Then, these generated ions are accelerated to high velocity towards the thruster exhaust by the electric field to generate thrust. On the thruster exterior, the ion beam is neutralized by electrons from the virtual cathode so that no charge builds up on the spacecraft's surface [2]. More details on Hall thruster operation and fundamentals can be found in [1–13].

Hall thrusters offer several benefits like simple design, high thrust-to-power ratio, high efficiency, improved performance, etc., which give them a clear advantage over other electric thrusters. For an input power range of 0.1 kW–20 kW, they can produce a few mN to 1 N of thrust and offers a specific impulse in the range of 1000s–3000s with more than 50% efficiency [14]. Hall thrusters can also adjust their thrust level and specific impulse by varying the discharge voltage and propellant mass flow rate, which makes them suitable for applications such as precision maneuvering, attitude control, station keeping and orbital raising [15]. In addition, plasma in a Hall thruster remains quasi-neutral, which eliminates the issue of space charge, allowing the Hall thruster to achieve higher thrust densities. Because of all these characteristics, the space community has shown great interest in Hall thrusters and they have been used successfully on many spacecraft for space missions and maneuvers.

Thrust is caused by a change in a substance's momentum as a result of a chemical reaction or an electrical principle. The thrust indicates how much force, in newtons (N), the propulsion system exert on the vehicle. Let us denote $\dot{m}_p$ as the mass flow rate, the exhaust velocity $\vec{U}_{ex}$ and g is the acceleration due to gravity, then spacecraft's thrust denoted by

$$T = \dot{m}_p \vec{U}_{ex} \tag{1}$$

The performance of thrusters is usually determined by thrust T, which is the total force undergone by the rocket. Thrust also has same unit as a force in newton, which shows the movement of the propulsion system. Thrust, is generated by the burning of fuel or by the electrostatic forces. The thrust $T = \dot{m}_p \vec{U}_{ex}$, if the mass flow rate is constant. The specific impulse I_{sp} is used to compare the efficiencies of different type of propulsion systems [2]. The specific impulse is expressed as $I_{sp} = \frac{T}{\dot{m}_p g}$. In general, the higher the specific impulse the less fuel is required. Therefore the specific impulse simplifies to $I_{sp} = \frac{\vec{U}_{ex}}{g}$. The specific impulse has the dimension of time and is a measure for the effective mission time of the thruster. The high value of the specific impulse reduces the mission time. If we denote the thrust efficiency η and the input power P_t, then these are related by

$$T = \frac{2\eta P_t}{I_{sp} g} \tag{2}$$

Tsiolkovsky rocket Eq. (1) can be read as

$$\Delta \vec{v} = \vec{v}_f - \vec{v}_i = \vec{U}_{ex} \ln\left(\frac{m_f}{m_f + m_p}\right) \tag{3}$$

The above Rocket equation defines the change in velocity of a spacecraft. It is clear that a higher $d\vec{v}$ demands more propellant. In terms of specific impulse, the above equation simplifies to

$$\Delta\vec{v} = \vec{v}_f - \vec{v}_i = I_{sp}g \ln\left(\frac{m_f}{m_f + m_p}\right) \tag{4}$$

We can now say that I_{sp} plays a key role in the design of a space mission propulsion system.

2. Description of the Hall thruster

This description of the Hall thruster is shown in **Figure 1**. The anode and cathode set up an axial electric field and magnetic coils create a radial magnetic field. First cathode starts producing a stream of electrons and these electrons are attracted by positive anode. When electrons are moving to anode, then at the channel exit they face of perpendicular electric and magnetic fields, these fields are more strong at channel exit. Due to these perpendicular fields, electrons trapped in an ExB drift and formed Hall current [1]. At this time Xenon gas is released from the anode, when neutral atom of gas reached at the channel exit, then electron collides with neutral atoms and ionized them. These ions are accelerated out of channel by electric field at the channel exit and this motion of ions imparts a reaction force on the thruster in reverse direction. The cathode is also used to neutral the ions charge so it produce a stream of electron to neutral the ions [1–10].

2.1 Stationary plasma thruster (SPT)

The wall material of this type of thruster is dielectric like borosil (BN-SiO2), boron nitride (BN) and alumina. This type of material has low secondary electron emission coefficient with Xenon ion interaction. Most of SPT use Xenon as a propellant because of its higher mass (131.3amu), lower first ionization potential, less toxicity, ionization cross section of ($\sim 2.310^{-6}$cm^2) and of its desirable thermodynamics properties [1, 10].

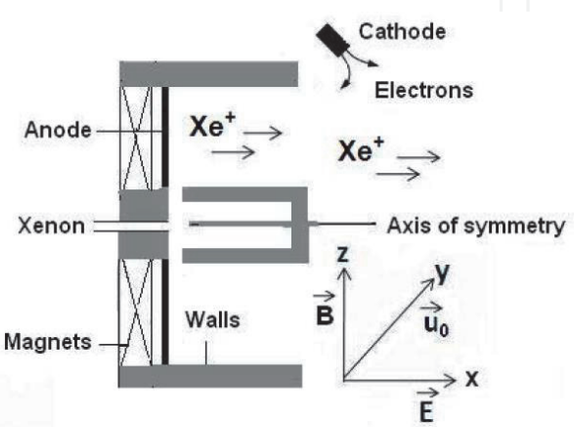


Figure 1.
Schematic diagram of a typical Hall plasma thruster.

2.2 Thruster with anode layer (TAL)

These types of thruster has metallic conducting walls and has narrow acceleration zone associated with the narrow electric field region near the anode. The ratio of channel width and channel depth in these thruster is 2:1. The conducting channel wall is negatively biased and it is a part of magnetic circuit so it prevent electron to move in direction of wall and repel them to ionization region and reduce electron power losses [1–10].

3. Components of a Hall thruster

The main components of a Hall thruster are body, magnetic coils, discharge channel, anode and cathode. The body of the Hall thruster provides better shape of external magnetic field, so it is normally made up of iron (steel). In this thruster a single thick disk shape annular discharge channel exist on the front face. To create better shape of magnetic field two type of magnetic coils are situated in the thruster channel. The inner coil is made of single reel and located radially inward in the channel and the outer coil is made of multiple reels and located radially outward in the channel. The magnetic coils and iron body made a magnetic circuit. The magnetic iron body of the thruster is separated from thruster discharge channel by walls and the material of these walls is metal or ceramic. The material of the anode is normally stainless steel, which avoids magnetic interaction and supply hardiness [1–10]. To set up an axial electric field in discharge channel of thruster a cathode is required and this cathode is normally hollow cathode with lanthanum hexaboride or barium oxide. The cathode completes the discharge circuit and work like an electron source. This description of the Hall thruster provides knowledge about the structure of thruster.

4. Hall current and thrust

As discussed earlier, there is an azimuthal electron drift in a Hall thruster channel, which is normal to both the applied electric field and generates a Hall current [1, 10]. Because of the collisions of the electrons with neutrals, electrons, ions and potential fluctuations in the plasma, generate the axial electron current density. The azimuthal E X B drift is given by

$$v_d = \frac{\vec{E} \times \vec{B}}{B^2} \approx \frac{E_r}{B_z} \tag{5}$$

The Hall current may be approximated by integrating the magnitude of E_r/B_z along the acceleration region and multiplying the result by the electron charge density and width. In mathematically, it can be read as

$$I_H \approx en_e \int_0^L \frac{E_r}{B_z} dx \approx \frac{ewn_e V_d}{B} \tag{6}$$

Here, w is the channel width and V_d is the voltage at cathode.

5. Channel length and scaling laws for Larmor radius

The ratio of electric and magnetic field is such that the ion's gyro radius is much larger than electron's gyro radius, so that ions are not magnetized inside the channel. The channel length is calculated by determining the Larmor radius of both the plasma species [10]. The motion of the moving charged particle under the electromagnetic fields defined as follows

$$\frac{m{v_\perp}^2}{r} = q(v_\perp \times B) \tag{7}$$

This gives the radius of gyration

$$r = \frac{mv_\perp}{qB} = \frac{v_\perp}{\Omega_c} \tag{8}$$

Here, $\Omega_c = \frac{qB}{m}$, is called the cyclotron frequency. If ions are accelerated through electrical potential $V_\perp$ (perpendicular to the magnetic field), then energy balance leads to $\frac{m{v_\perp}^2}{2} = qV_\perp$.

This implies to

$$v_\perp = \sqrt{\frac{2qV_\perp}{m}} \tag{9}$$

These above equations gives the larmor radius in terms of the applied potential

$$r = \frac{1}{B}\sqrt{\frac{2mV_\perp}{q}} \tag{10}$$

The magnitudes of the fields are such that $r_i >> L >> r_e$, where L (~6 cm) is the length of the acceleration channel. For a typical Hall thruster, Larmor radius for electrons (~0.13 cm) and ions (~180 cm) corresponds to the radial magnetic field strength of order 150 G and energy 300 eV.

Despite many successful applications of Hall thrusters, some aspects of their operation are still poorly understood. One notable problem is the anomalous electron mobility [16, 17] and plasma sheath, which is far above the classical collisional values. It has been established that the inhomogeneous plasma under the electromagnetic fields is not in the thermodynamically equilibrium state [17–20]. The equilibrium E × B electron drift, ion flow rate, plasma and magnetic field gradients are all sources of plasma instabilities in Hall plasmas. Hall plasmas devices with ExB electron drift demonstrate wide range of turbulent fluctuations. These fluctuations are probably the reason of the observed anomaly in the electron transport across the magnetic field [21–23] and other nonlinear phenomena (coherent rotating spoke) [24–26]. Understanding of the mechanisms of the coherent structures and anomalous transport requires the detailed study of linear instabilities in Hall plasma devices. These instabilities are also considered to be a principal source of anomalous transport in toroidal magnetic confinement devices [2].

6. Oscillations and instabilities in Hall thrusters

If free energy is available in the system and even though system is in equilibrium in the sense that all the forces are in balance, then these oscillations can grow at the

cost of free energy and hence instabilities can take place. There are different types of instabilities that depend on different conditions. For proper description of a particular instability, one should be able to define the mode of the growing wave, the nature of the growth and the source of the free energy. Instabilities are mainly classified into four groups, namely streaming instabilities, Rayleigh–Taylor instabilities, universal instabilities and kinetic instabilities.

When there is any kind of perturbation, the free energy available excites the waves and the plasma waves no longer remains in thermal equilibrium. Even though there exist an equilibrium because all the forces are balanced and there is no net force and it is possible to find a time independent solution to the wave. Perturbation makes the plasma waves unstable, which is always a motion that brings the plasma closer to true thermodynamic equilibrium by decreasing the free energy. Instabilities may be classified according to the type of free energy available to drive them. Few of them has been explained below.

6.1 Streaming instability

This type of instability occurs, when either a current or a beam of energetic particles is driven through plasma so that the different species of particles have drifts relative to one another. This drift energy attempt to excite waves and oscillation. This energy is acquired at the loss of the drift energy, which is in the unperturbed state.

6.2 Rayleigh–Taylor instabilities

In this kind of instability, the plasma has a sharp boundary or a density gradient, so that it does not remain uniform. In addition to this, an external, non-electromagnetic force is applied into the plasma. This force is responsible for driving the instability in plasma. This analogy can be realized in an inverted glass of water. Though the plane interface between the air and the water is in the state of equilibrium, where the air pressure support the weight of the water. Any ripple arising in the surface of water tend to grow at the loss of potential energy in the influence of gravitational field. Whenever a light fluid supports a heavy fluid this things happen, which is quite known in the field of hydrodynamics [1].

6.3 Universal instabilities

A plasma is hardly present in perfect thermodynamic equilibrium, when it is confined by gravitational field or an electric field (driving forces). The plasma is expanded by plasma pressure and an instability is driven by the expansion energy. Any finite plasma always contains this type of free energy and the waves, which comes out as a result are called universal instabilities.

6.4 Kinetic instabilities

Generally, the velocity distributions are assumed to be Maxwell-Boltzmann in fluid theory. If there is a case, where distributions are not Maxwell-Boltzmann, then there may be a departure from thermodynamic equilibrium and this anisotropy of the velocity distribution drive the kinetic instabilities.

6.5 Streaming instabilities

These kind of instabilities occur, when the plasma particles streams with their relative drift, which may be driven due to the travel of charge particle beam or

internal driven current. For example, the two stream instability is due to the relative drift of ion and electron streams.

6.6 Electromagnetic resistive instability

These instabilities have been investigated in various positions of the acceleration channel of the thruster. The effect of radial magnetic field, thermal motions of plasma particles and electron collisions can induce time varying fields in the discharge oscillations. This can prompt an electromagnetic resistive instability in the Hall thruster. In this chapter, we derive the dispersion relation for the electromagnetic instabilities in a Hall thruster and conditions for the instability.

6.7 Oscillations and instabilities in Hall thrusters

There are numerous types of oscillation found in thrusters which propagates in azimuthally and axially direction ranging from a few kHz to tens of MHz [1, 10]. These oscillations may reduce the specific impulse and the efficiency of a Hall thruster. These disturbances can also limit the operating life of a Hall thruster and therefore, suppression of this oscillation has become an essential task for Hall thrusters. These fluctuations are responsible for electron transport across magnetic field lines, performance and ionization of propellant [27–30]. The magnitude of these oscillations strongly depend on the magnetic field, location of the cathodes, the discharge voltage and the mass flow rate.

Low frequency oscillation, frequently referred to as the breathing mode, is intimately tied to the details of propellant ionization and eventual ion acceleration and manifests itself as a strong 10–30 kHz oscillation in the thruster discharge current. Breathing mode models suggest the presence of a propagating ionization front traversing the channel of the thrusters [31]. Benítez and Ahedo investigated the axial-azimuthal instabilities in the global discharge region of a Hall-thruster to identify dominant mode (develops in the near plume at 1–5 MHz) and subdominant mode (develops near the anode100–300 kHz) [32]. Lafleur *et al*. studied transport effects of the electron drift instability in Hall-effect Thrusters [33]. Fan *et al*. studied the effects of the peak magnetic field position on Hall thruster discharge characteristics [34]. Sekine *et al*. investigated the spatially and temporally resolved ion flow measurements inside the plasma source of an inductive radio frequency plasma thruster [35]. Puerta *et al*. generalized non-ideal treatment and growth rates analysis of drift waves instabilities in a collisions-free magnetized dusty plasma [36]. The electrostatic dispersion relation for an unbounded homogeneous plasma in the presence of unmagnetized ions, magnetized electrons and an applied magnetic field has been solved numerically by Mikellides and Ortega in the near-plume of a magnetically shielded Hall thruster [37]. Tomilin and Ivan Khmelevskoi studied the influence of kinetic effects on dispersion properties of high-frequency perturbations in Hall thruster plasmas [38]. Marcovati *et al*. reported the dynamic behavior of gradient-driven drift waves in a strongly magnetron discharge in multi ion plasma [39]. Litvak and Fisch [40] investigated resistive instabilities in a Hall plasma and found that plasma perturbations in the acceleration channel are unstable in the presence of collisions. Fernandez *et al*. [41] did simulations for resistive instabilities. Marusov et al. [42] modeled the stability of gradient-drift waves in a Hall-type plasma using two-fluid ideal magnetohydrodynamics. Ducrocq et al. [43] studied high-frequency electron drift instability, where they derived three-dimensional dispersion relation for a model of a crossed electric and magnetic field configuration existing in the Hall thruster. Litvak and Fisch [44] have analyzed gradient driven Rayleigh type instabilities in a Hall thruster using two fluid

hydrodynamic equations. Kapulkin and Guelman [45] investigated low frequency instability in near anode region of a Hall thruster, where they obtained that the instability can be responsible for the enhanced transfer of the electrons between the ionization region and the anode. Choueiri [46] has quantitatively discussed the nature of oscillations in the 1 kHz–60 MHz frequency range observed during operation of Hall thrusters. Various plasma parameters measured inside the accelerating channel of a typical Hall thruster were used to evaluate the various stability criteria and dispersion relations of oscillations [46].

At small amplitudes, the oscillations can be considered a part of normal operation with no significant effect on operation. At large amplitudes, the oscillations can severely and adversely affect operation. The details of these oscillation are given in **Table 1**.

Lakhin *et al.* have developed the effects of finite electron temperature on gradient drift instabilities in partially magnetized plasmas in the frequency range $\omega_{Bi} \ll \omega \ll \omega_{Be}$ driven by the equilibrium current perpendicular to the magnetic field [56]. Romadanov *et al.* [57] studied the structure of nonlocal gradient-drift instabilities in Hall E × B discharge plasma. Koshkarov *et al.* calculated the linear and nonlinear nonlocal instability of axial lower-hybrid modes in plasma under the influence of ion flow rate [58]. Smolyakov *et al.* have used fluid theory and performed the simulations of instabilities, turbulent transport and coherent structures in magnetized plasmas [59]. Singh and Malik [60, 61] investigated that temperature of the ion and drift velocity profiles of the electron modifies the conditions

Type	Description	Ranges of frequencies
Spoke type	Spoke type oscillations are propagating in the azimuthal direction at low discharge voltages [47, 48].	15–35 kHz
Breathing mode	Discharge-current low-frequency oscillations [49]	Range of 10–100 kHz
Contour oscillations	These are longitudinal oscillations connected with an instability in the location of the ionization region and can have very large amplitude [50–53]. Contour oscillations depend on the parameters of the discharge power supply circuit.	1–30 kHz (correspond to the transit time for a neutral propellant atom)
Ionization oscillations	These oscillations are caused from the ionization front propagating irregularly around the circumference of the discharge channel [47, 52].	10–100 kHz.
Flight oscillations	These oscillations are also called ionization flight oscillations, because they are determined by the change of ionization rate due to the delay of particle appearance, from one region to another. The analysis is based on the concept that plasma particles are delayed in being transferred from one region to other [54].	100 kHz up to 10 MHz (correspond with the transit time for an ion)
High frequency oscillations	The amplitude of these oscillations is smaller and these are azimuthal waves generated near the exit part of the thruster [55].	1–100 MHz
Super high frequency oscillations	These oscillations are connected with the development of electron layers in the plasma and the formation of flows of fast overheated electrons and have the smallest amplitude [55].	Few GHz

Table 1.
Types and frequency range of oscillations in Hall thrusters.

for Rayleigh type instability under the effects of thermal motions of ions and plasma resistivity induces resistive instabilities (electrostatic and electromagnetic) [62–65] associated with azimuthal and axial directions. Yadav et al. presented the model for relativistic electron-beam assisted growth of oscillating two-stream instability [66]. Aria and Malik [67] have investigated the propagating modes, instabilities and plasma sheath formed on the outer surface of a spacecraft. The detailed physical picture of the processes in the thruster is very complex. It includes a whole series of phenomena, such as stabilization of the flow in cross-fields. Becatti et al. investigated the properties of plasma oscillations in the exterior region of a high-current hollow cathode [68].

7. Magnetic field profiles and erosion problems

Magnetic field is an important parameter, which affect the performance and operation of Hall thruster. The erosion on the channel walls and on the electrodes can be minimized by accelerated beam of ions to a narrower beam width and by use of appropriate profile of magnetic field. The radial magnetic field causes the erosions of the walls, so new topology of magnetic field 'lens' is proposed by Morozov [69]. By using magnetic shielding technique, the discharge chamber erosion rate can be reduced by orders of magnitude [70]. Morozov and Lebedev proposed a magnetic field lens to focus the plasma beam [71]. Morozov et al. have designed a lens-type magnetic field with a zero magnetic point to make the plume divergence half angle only 10° in SPT-ATON Hall thruster [72]. Hofer et al. showed that the performance of the Hall thruster can be enhanced by reducing the divergence of the plume that could damage the solar panels and other parts of the satellite [73]. Hofer et al. used magnetic field to control the unmagnetized ion beam that formed in Hall thruster. By controlling ion beam the wall erosion was reduced to 2–3 order by ion bombardment [74]. Huang et al. studied the effect of background pressure on performance and plume of NASA's High Voltage Hall Accelerator Hall thruster [75]. Their result shows that discharge current and thrust are increases with pressure and ion beam current, ion energy per charge, plum divergence decreases with increasing background pressure.

Liu et al. studied the effect of azimuthally electron drift on sheath profile and anomalous erosion in thrusters. Their results show that azimuthally electron drift induce sheath oscillations and it can produce an asymmetric sheath structure. To simulate the azimuthally erosion evolution, an erosion modal is used and it has been concluded that the azimuthally asymmetric ion sputtering is responsible for an asymmetric erosion profile [76]. Kim studied the ionization processes and ion dynamics in the accelerating channel to determine the stationary plasma thrusters performance levels [54]. Choueiri theoretically studied the difference between stationary plasma thruster and thruster with anode layer by measuring the temperature of secondary electron emission from the walls of thruster [77]. Hong et al. studied the effect of wall grooves on Hall thruster discharge to improve the performance of Hall thruster. If wall grooves are present in ionization region it increases near wall conductivity and decrease electron transient time, thrust and efficiency [78]. Ding et al. studied the discharge current and stability in graphite walls and BN-SiO_2 walls for magnetic shielded and unshielded thruster. Their result shows that magnetic shielded thruster does not show change in stability and discharge current but 25% discharge current increases in unshielded thruster [79]. Experimental results and PIC simulation show that oblique channel's specific impulse, anode efficiency, thrust, propellant utilization and ionization in plume region is improved 20% rather than the straight channel thruster [80]. Olano et al. studied the effect of

magnetic field configuration on thruster performance and plasma discharge by proposing three types of configurations: (A) nominal, (B) orthogonal magnetic field and (C) high magnetic field [80, 81]. Garrigues et al. did PIC simulations and shows that in a Hall thruster electric discharge produce due to wall-plasma interaction and wall of thruster channel is reduced due to interaction with ions [82]. The electrostatic and magnetic probes are used to investigate the electromagnetic fluctuations and coherent magnetohydrodynamic azimuthal modes in thruster [68].

8. Introduction to electromagnetic instabilities and their dispersion relations

The resistive instability is driven by coupling to a dissipative process. Due to the collisions between the electrons and neutral particles, resistive instability can occur in the acceleration channel of the Hall thruster. This instability occurs due to the interaction of the wave with the electrons' flow in the presence of electron collisions. The two major problems in plasma confinement are equilibrium and stability of plasma. The system in an equilibrium state if all the forces, which act on a system are balanced but stability and instability of the equilibrium can be assured by giving some perturbations to the equilibrium state. The stable and unstable state of equilibrium depend on small perturbation whether the perturbations are damped or amplified. For small perturbations, equilibrium is non- linear but stability can be linearized.

9. Plasma model and basic equations for purely azimuthal waves

For the case of small amplitude perturbations and wavelengths much smaller than the scale lengths of inhomogeneities, the analysis of linearization can be applied. In the simplest approach, we consider the x- axis is taken along the axis of the thruster and the z-axis is taken along the radius of the thruster. The direction the magnetic field $\vec{B}$ is along the z- axis. The y- axis is taken correspond to the azimuthal direction. Consistent to the fluid approach, we write below the basic fluid equations

$$\frac{\partial n_j}{\partial t} + \vec{\nabla} \cdot \left(\vec{v}_j n_j \right) = 0 \tag{11}$$

where n_j is the mass density and $\vec{v}_j$ is the velocity of species j (j = i, e). The momentum equations for electrons and ions are

$$\frac{\partial \vec{v}_e}{\partial t} + \left(\vec{v}_e \cdot \vec{\nabla} \right) \vec{v}_e + v \vec{v}_e = -\frac{e\vec{E}}{m} - \frac{e}{m} \left(\vec{v}_e \times \vec{B} \right) \tag{12}$$

$$\frac{\partial \vec{v}_i}{\partial t} + \left(\vec{v}_i \cdot \vec{\nabla} \right) \vec{v}_i = -\frac{e\vec{E}}{M} \tag{13}$$

9.1 Linearization of fluid equations

To linearize all the equations, let us write $n_i = n_0 + n_{i1}$, $\vec{v}_i = \vec{v}_{i1} + \vec{v}_0$, $\vec{B} = \vec{B}_1 + \vec{B}_0$ and $\vec{E} = \vec{E}_1 + \vec{E}_0$. The unperturbed density is taken as n_0, electric field

(magnetic field) as $\vec{E}_0(\vec{B}_0)$ and the perturbed value of the electric field (magnetic field) is taken as $\vec{E}_1(\vec{B}_1)$. Here, we consider the perturbed densities for ions and electrons as n_{i1} and n_{e1} velocities as $\vec{v}_{i1}$ and $\vec{v}_{e1}$ indicated by subscript 1 along with their unperturbed values as v_0 and u_0 in the x- and y-directions respectively. In view of small variations of both the density and magnetic field along the channel, the plasma inhomogeneities are neglected. The oscillations of the perturbed on and electron densities are taken small enough $(n_{i1}, n_{e1} << n_0)$ so that the collisional effect due to the velocity perturbations dominate over the one due to the density perturbation. Since $\vec{v}_0$ and u_0 are constant, the terms $\left(\vec{v}_0 \cdot \vec{\nabla}\right)n_0$, $n_0\left(\vec{\nabla} \cdot \vec{v}_0\right)$ and $n_1\left(\vec{\nabla} \cdot \vec{v}_0\right)$ are equal to be zero. Further the terms $\left(\vec{v}_1 \cdot \vec{\nabla}\right)n_1$, and $n_1\left(\vec{\nabla} \cdot \vec{v}_1\right)$ are neglected as they are quadratic in perturbation.

The linearizations of the above eqation leads to

$$\left(\frac{\partial}{\partial t} + u_0\frac{\partial}{\partial y} - v\right)\vec{v}_{e1} + \frac{e}{m}\left(\vec{E}_1 + \vec{v}_{e1} \times \vec{B} + \vec{u}_0 \times \vec{B}_1\right) = 0 \tag{14}$$

$$\left(\frac{\partial}{\partial t} + v_0\frac{\partial}{\partial x}\right)\vec{v}_{i1} - \frac{e\vec{E}_1}{M} = 0 \tag{15}$$

$$\frac{\partial n_{e1}}{\partial t} + u_0\frac{\partial n_{e1}}{\partial y} + n_0\left(\vec{\nabla} \cdot \vec{v}_{e1}\right) = 0 \tag{16}$$

$$\frac{\partial n_{i1}}{\partial t} + v_0\frac{\partial n_{i1}}{\partial x} + n_0\left(\vec{\nabla} \cdot \vec{v}_{i1}\right) = 0 \tag{17}$$

9.2 Dispersion equation and growth rate of azimuthal waves

We take the variation of oscillating quantities in azimuthal direction as $\sim \exp(i\omega t - iky)$. The linearized Eqs. (14)–(17) are used and the density and velocity perturbations are expressed in terms of the electric field as

$$v_{ex1} = \frac{eE_y}{m\Omega} + -i\frac{eE_x\hat{\omega}}{m\Omega^2} \tag{18}$$

$$v_{ey1} = \frac{u_0B_1}{B} - \frac{eE_x}{m\Omega} - \frac{ieE_y\hat{\omega}}{m\Omega^2} \tag{19}$$

From Eq. (15)

$$v_{ix1} = -\frac{ieE_x}{M\omega} \tag{20}$$

$$v_{iy1} = -\frac{ieE_y}{M\omega} \tag{21}$$

From Eqs. (13) and (14)

$$n_{e1} = -\frac{ekn_0\left(i\hat{\omega}E_y + \Omega E_x\right)}{m\Omega^2(\omega - ku_0)} \tag{22}$$

$$n_{i1} = -\frac{ien_0kE_y}{M\omega^2} \tag{23}$$

The x-component of the perturbed current density

$$J_x = en_0(v_{ix1} - v_{ex1}) + en_{i1}v_0 e \tag{24}$$

and the y-component of the perturbed current density

$$J_y = en_0\left(v_{iy1} - v_{ey1}\right) - en_{e1}u_0 \tag{25}$$

9.3 Conductivity tensor

From the Maxwell's equation, we have

$$\nabla \times \vec{B} = \mu_0 \vec{J} + \mu_0 \epsilon_0 \frac{\partial \vec{E}}{\partial t} \tag{26}$$

or

$$\vec{J} = \frac{\nabla \times \vec{B}}{\mu_0} - \frac{\partial \vec{E}}{\partial t} \tag{27}$$

Faraday's law gives the relationship between changing electric and magnetic field as

$$\nabla \times \vec{E} = -\frac{\partial \vec{B}}{\partial t} \tag{28}$$

For a plane electromagnetic wave

$$\vec{E} = \overrightarrow{E_0} e^{j(\vec{k}.\vec{r} - \omega t)} \tag{29}$$

Where $\vec{E}$ is the electric field, $\vec{B}$ is the magnetic field, j represents the complex number, $\vec{k}$ is the wave vector, t is the time, $\overrightarrow{E_0}$ and $\overrightarrow{B_0}$ is complex magnitude of electric and magnetic field. Then ∇ operation gives ik and $\frac{\partial}{\partial t}$ gives $-i\omega$. Substituting these operators Faraday's law become

$$\vec{k} \times \vec{E} = \omega \vec{B}$$

or

$$\vec{B} = \frac{\vec{k} \times \vec{E}}{\omega} \tag{30}$$

9.4 Permittivity tensor

From Maxwell's equations, we get

$$\vec{D} = -\frac{\vec{k} \times \vec{k} \times \vec{E}}{\omega^2 \mu_0} \tag{31}$$

which on expansion will give

$$\begin{bmatrix} D_x \\ D_y \\ D_z \end{bmatrix} = \frac{1}{\omega^2 \varepsilon_0 \mu_0} \begin{bmatrix} k^2 - k_x^2 & -k_x k_y & -k_x k_z \\ -k_y k_x & k^2 - k_y^2 & -k_y k_z \\ -k_z k_x & -k_z k_y & k^2 - k_z^2 \end{bmatrix} \begin{bmatrix} E_x \\ E_y \\ E_z \end{bmatrix} \tag{32}$$

Then permittivity tensor will be

$$\varepsilon_r = \frac{1}{\omega^2 \varepsilon_0 \mu_0} \begin{bmatrix} k^2 - k_x^2 & -k_x k_y & -k_x k_z \\ -k_y k_x & k^2 - k_y^2 & -k_y k_z \\ -k_z k_x & -k_z k_y & k^2 - k_z^2 \end{bmatrix}$$

In general

$$\varepsilon_{rij} = \frac{1}{\omega^2 \varepsilon_0 \mu_0} \left[k^2 \delta_{ij} - k_i k_j \right] \tag{33}$$

But for a pure dielectric medium $k = \frac{\omega}{c}\sqrt{\varepsilon_r}$ and we will get

$$\varepsilon_r = \begin{bmatrix} \varepsilon_{rr} - \varepsilon_{rx} & -\varepsilon_{rx}\varepsilon_{ry} & -\varepsilon_{rx}\varepsilon_{rz} \\ -\varepsilon_{ry}\varepsilon_{rx} & \varepsilon_{rr} - \varepsilon_{ry} & -\varepsilon_{ry}\varepsilon_{rz} \\ -\varepsilon_{\mathrm{rz}}\varepsilon_{rx} & -\varepsilon_{rz}\varepsilon_{ry} & \varepsilon_{rr} - \varepsilon_{rz} \end{bmatrix}$$

Then, the Maxwell's equations are used in view of the perturbed electric and magnetic fields of the electromagnetic wave, and the plasma dielectric tensor ε_{ij} is obtained as

$$\varepsilon_{ij} E_j = E_j \delta_{ij} + \frac{j_i(E_j)}{i\omega\varepsilon_0} \tag{34}$$

Finally, the wave equation $\left(k^2 \delta_{ij} - k_i k_j - \frac{\omega^2}{c^2}\varepsilon_{ij}\right) E_j = 0$ is written in the following form

$$k^2 \varepsilon_{yy} - \frac{\omega^2}{c^2}\left(\varepsilon_{xx}\varepsilon_{yy} - \varepsilon_{xy}\varepsilon_{yx}\right) = 0 \tag{35}$$

Where, the components of the dielectric tensor are obtained from Eq. (34) with the help of the Eqs. (24) and (25)

$$\varepsilon_{xx} = \frac{(\omega - k u_0){\omega_e}^2}{\omega \Omega^2} + 1 - \frac{{\omega_i}^2}{\omega^2} \tag{36}$$

$$\varepsilon_{xy} = \frac{i{\omega_e}^2}{\omega\Omega} - \frac{{\omega_i}^2 k v_0}{\omega^3} \tag{37}$$

$$\varepsilon_{yx} = \frac{{\omega_e}^2}{i\omega\Omega} + \frac{{\omega_e}^2 k u_0 \Omega}{i\Omega^2 \omega(\omega - k u_0)} \tag{38}$$

$$\varepsilon_{yy} = \frac{{\omega_e}^2 k u_0 \hat{\omega} k}{\Omega^2 \omega(\omega - k u_0)} - \frac{{\omega_i}^2}{\omega(\omega - k u_0)} + \frac{{\omega_e}^2 \hat{\omega}}{\omega\Omega^2} + 1 \tag{39}$$

By substituting these components into Eq. (35) we get the following cumbersome analytical expression of the dispersion relation of electromagnetic waves propagating in magnetized plasma [40].

$$\frac{k^2c^2}{\omega^2} = \frac{(\omega - ku_0){\omega_e}^2}{\omega\Omega^2} + 1 - \frac{{\omega_i}^2}{\omega^2} + \frac{\left\{\frac{{\omega_e}^2}{i\omega\Omega} + \frac{{\omega_e}^2 ku_0\Omega}{i\Omega^2\omega(\omega - ku_0)}\right\}\left\{\frac{{\omega_e}^2}{i\omega\Omega} - \frac{{\omega_i}^2 kv_0}{\omega^3}\right\}}{\left\{\frac{{\omega_e}^2 ku_0\hat{\omega}k}{\Omega^2\omega(\omega - ku_0)} - \frac{{\omega_i}^2}{\omega(\omega - k_y u_0)} + \frac{{\omega_e}^2\hat{\omega}}{\omega\Omega^2} + 1\right\}} \tag{40}$$

9.5 Typical parameters of Hall thrusters

The values and ranges of some typical parameters are given in **Table 2**.

9.6 Numerical results and discussion

We solve the dispersion Eq. (40) to find out complex root by using typical values of the magnetic field, azimuthal wave number, collision frequency, electron drift velocity, ion drift velocity and electron temperature. Then the effect of these parameters on the growth γ of the electromagnetic wave is studied in **Figures 1–4**.

Figure 2 shows that the growth rate of the wave get enhanced for the larger values of the drift velocity of the electrons [64]. Since the drift velocity can be correlated with the discharge voltage, so it can be said that the growth rate is increased with the discharge voltage. Esipchuk and Tilinin [83] also reported the proportionality of the frequency of drift instability to the discharge voltage. The increase in the growth rate may be attributed to the strong coupling between the electric field and electron current [84].

Figure 3 shows the variation of growth rate under the effect of collisional frequency. It is seen that the wave grows at a faster rate in the presence of more electron collisions. Since the stronger resistive coupling of the oscillations to the electrons' closed drift requires the electron collisions, it is obvious that this instability grow faster in the presence of higher collision frequency. Similar results were also reported in the simulation studies of resistive instability by Fernandez *et al.* [41] that the growth rate is directly proportional to the square root of the collision frequency.

The dependence of growth rate on the magnetic field is shown in **Figure 4**, where it is observed that the wave grows faster in the presence of strong magnetic

Property	Typical value	Property	Typical value
Inner diameter	60 mm	Neutral velocity	300 m/s
Outer diameter	100 mm	Electron temperature	5-10 eV
Plasma density	$10^{17}/m^3$	Ion temperature	1-5 eV
Neutral density	$10^{18}/m^3$	Neutral temperature	0.9 eV
Ion velocity	10^4 m/s	Debye length	10^{-5} m
Collision mean free path	1 m		

Table 2.
Typical values of parameters used in Hall thruster.

DOI: http://dx.doi.org/10.5772/intechopen.99883

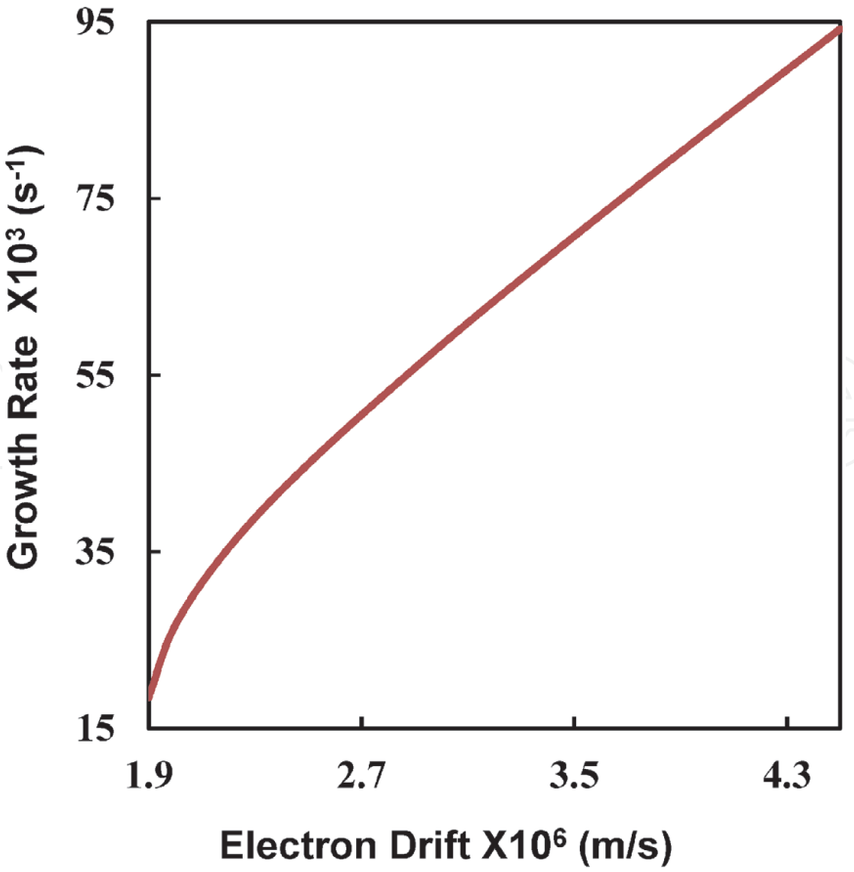


Figure 2.
The dependence of growth rate with electron drift velocity.

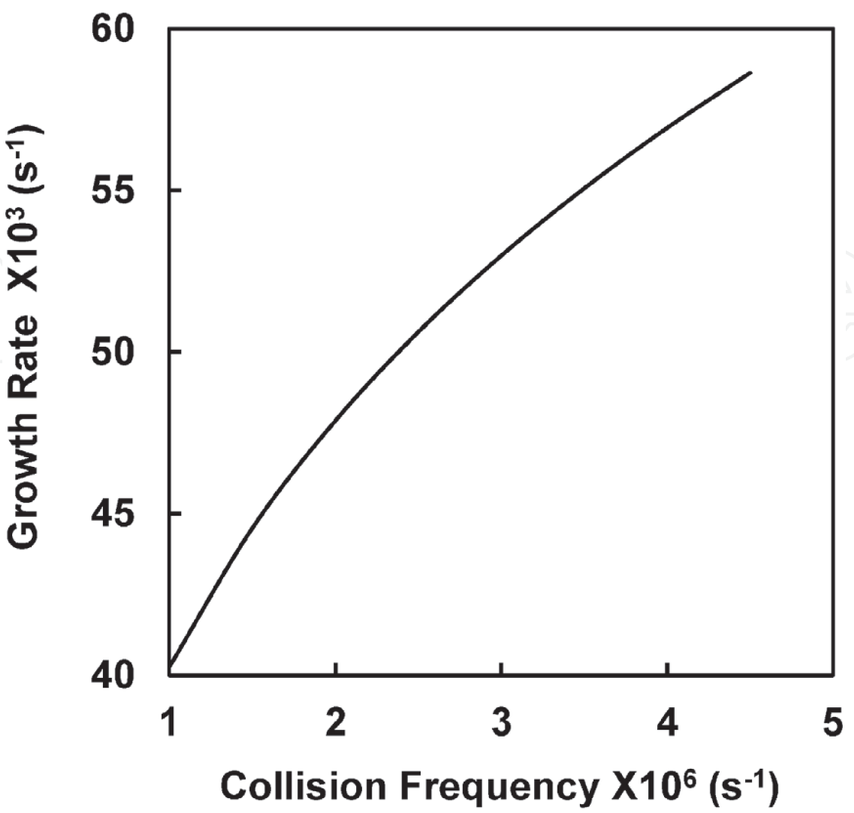


Figure 3.
Variation of growth rate with collision frequency.

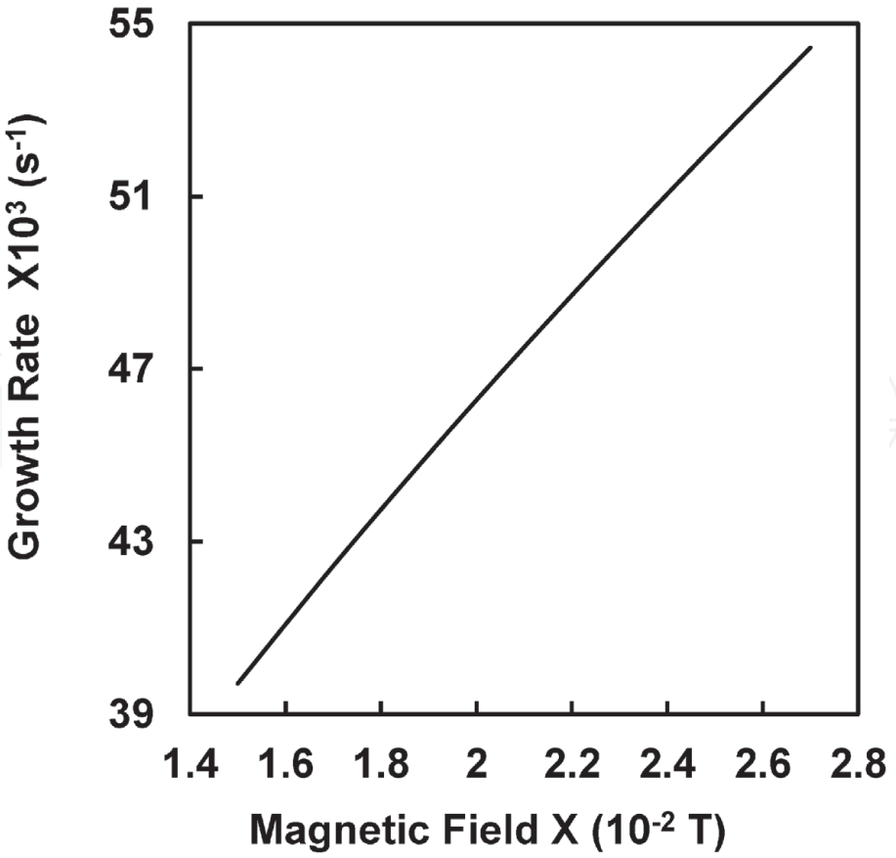


Figure 4.
Variation of growth rate with magnetic field.

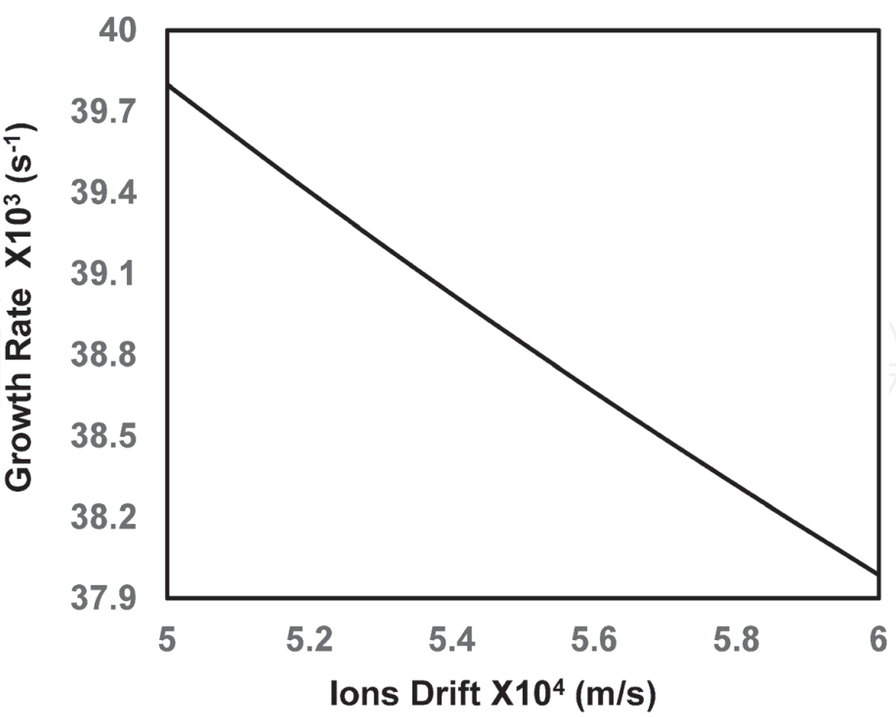


Figure 5.
Dependence of growth on ion drift velocity.

field. The growth rate of the wave gets suppressed under the larger drift of the ions as shown in the **Figure 5**. Since in the presence of their large drift, the ions try to diminish the transverse oscillations of the electrons in the x-direction.

10. Results and the discussion

The different aspects of the Hall thrusters have been reviewed in this chapter along with future challenges related to the performance and efficiency. The different types of turbulence and oscillation with frequency ranges are also summarized. Hall thruster Plasma support electrostatic and electromagnetic waves under the influence of resistive effects. Therefore the waves (electrostatic and electromagnetic) propagating in azimuthal direction in a Hall thruster channel are found to be unstable due to the resistive coupling to the electrons' closed drift in the presence of collisions. The theoretical model for the propagation of electromagnetic instability is derived in a Hall thrusters. The dispersion relation for the electromagnetic instability is derived analytically. The dispersion relation is solved numerically with the help of MATLAB to study the growing and propagating modes. The dominated modes are plotted to observe the behaviors of the instability.

Acknowledgements

The University Grants Commission (UGC), New Delhi, India is thankfully acknowledged for providing the startup Grant (No. F. 30-356/2017/BSR).

Author details

Sukhmander Singh[1*], Bhavna Vidhani[2] and Ashish Tyagi[3]

1 Plasma Waves and Electric Propulsion Laboratory, Department of Physics, Central University of Rajasthan, Kishangarh, India

2 Department of Physics and Electronics, Hansraj College, University of Delhi, Delhi, India

3 Department of Physics, Swami Shraddhanand College, University of Delhi, Delhi, India

*Address all correspondence to: sukhmandersingh@curaj.ac.in

IntechOpen

© 2021 The Author(s). Licensee IntechOpen. This chapter is distributed under the terms of the Creative Commons Attribution License (http://creativecommons.org/licenses/by/3.0), which permits unrestricted use, distribution, and reproduction in any medium, provided the original work is properly cited. CC BY

References

[1] Goebel DM, Katz I. Fundamentals of Electric Propulsion: Ion and Hall Thrusters. New York: Wiley; 2008

[2] Charles C. Plasmas for spacecraft propulsion. J. Phys. D Appl. Phys. 2009; **42**:163001

[3] Mozouffre, S. Electric propulsion for satellites and spacecraft: Established technologies and novel approaches. Plasma Sources Sci.Technol. 25, 033002 (2016).

[4] Levchenko I et al. Recent progress and perspectives of space electric propulsion systems based on smart nanomaterials. Nat. Commun. 2018;**9**:879

[5] Takahashi K. Helicon-type radiofrequency plasma thrusters and magnetic plasma nozzles. Rev. Mod. Plasma Phys. 2019;**3**:3

[6] Rovey JL, Lyne CT, Mundahl AJ, Rasmont N, Glascock MS, Wainwright MJ, Berg SP. Review of multimode space propulsion. Progress in Aerospace Sciences. 2020;118:100627(1-27).

[7] Brown NP, Walker ML. Review of plasma-induced Hall thruster erosion. Applied Sciences. 2020 Jan;10(11):3775 (1-18).

[8] O'Reilly D, Herdrich G, Kavanagh DF. Electric Propulsion Methods for Small Satellites: A Review. Aerospace. 2021; 8:1-30. Doi.org/ 10.3390/aerospace8010022

[9] Levchenko I, Xu S, Mazouffre S, Lev D, Pedrini D, Goebel D, Garrigues L, Taccogna F, Bazaka K. Perspectives, frontiers, and new horizons for plasma-based space electric propulsion. Physics of Plasmas. 2020; Feb 3;27(2):020601.

[10] Zhurin VV, Kaufman HR, Robinson RS. Physics of closed drift thrusters. Plasma Sources Science and Technology. 1999;**8**(1):R1

[11] Singh S. Evolutions of Growing Waves in Complex Plasma Medium. IntechOpen, London, United Kingdom, Nov: In edited book Engineering Fluid Mechanics; 2020

[12] Singh S. Dynamics of Rayleigh-Taylor Instability in Plasma Fluids. In the edited book Engineering Fluid Mechanics. IntechOpen, London, United Kingdom, April 15th 2020

[13] Singh S. Hall Thruster: An Electric Propulsion through Plasmas. In the edited book Plasma Science IntechOpen, London, United Kingdom, March 2nd 2020

[14] Boeuf, Jean-Pierre. Tutorial: Physics and modeling of Hall thrusters. Journal of Applied Physics 121.1 (2017): 011101.

[15] Warner, Noah Zachary. Theoretical and experimental investigation of Hall thruster miniaturization. Diss. Massachusetts Institute of Technology, 2007.

[16] A. B. Mikhailovskii, Theory of Plasma Instabilities, Vol. 1, Instabilities of a Homogeneous Plasma (Springer, New York, 1974).

[17] O. Buneman, Instability, turbulence, and conductivity in current-carrying plasma, Phys. Rev. Lett. 1(1), 8 (1958).

[18] O. Buneman, Excitation of field aligned sound waves by electron streams, Phys. Rev. Lett. 10(7), 285 (1963).

[19] D. T. Farley, A plasma instability resulting in field-aligned irregularities in ionosphere, J. Geophys. Res. 68(22), 6083 (1963).

[20] A. Simon, Instability of a partially ionized plasma in crossed electric and

magnetic fields, Phys. Fluids 6(3), 382 (1963).

[21] Keidar M, Beilis II. Electron transport phenomena in plasma devices with ExB drift. IEEE Transactions on Plasma Science. 2006 Jun 19;**34**(3): 804-814

[22] Hagelaar GJ, Bareilles J, Garrigues L, Boeuf JP. Role of anomalous electron transport in a stationary plasma thruster simulation. Journal of Applied Physics. 2003 Jan 1;**93**(1):67-75

[23] Adam JC, Boeuf JP, Dubuit N, Dudeck M, Garrigues L, Gresillon D, et al. Physics, simulation and diagnostics of Hall effect thrusters. Plasma Physics and Controlled Fusion. 2008 Nov 5; **50**(12):124041

[24] Ellison CL, Raitses Y, Fisch NJ. Cross-field electron transport induced by a rotating spoke in a cylindrical Hall thruster. Physics of Plasmas. 2012 Jan 12;19(1):013503.

[25] Griswold ME, Ellison CL, Raitses Y, Fisch NJ. Feedback control of an azimuthal oscillation in the E× B discharge of Hall thrusters. Physics of Plasmas. 2012 May 25;19(5):053506.

[26] Alvarez-Laguna A, Magin T, Massot M, Bourdon A, Chabert P. Plasma-sheath transition in multi-fluid models with inertial terms under low pressure conditions: Comparison with the classical and kinetic theory. Plasma Sources Science and Technology. 2020; 29:025003.

[27] Mandal D, Elskens Y, Lemoine N, Doveil F. Cross-field chaotic transport of electrons by E×B electron drift instability in Hall thruster. Physics of Plasmas. 2020; 27:032301.

[28] Smolyakov A, Zintel T, Couedel L, Sydorenko D, Umnov A, Sorokina E, et al. Anomalous electron transport in one-dimensional electron cyclotron drift turbulence. Plasma Physics Reports. 2020;**46**:496-505

[29] Oland E, Kristiansen R, Nicklasson PJ. Combined chemical and electric thruster solution for attitude control. In 4th International Conference on Recent Advances in Space Technologies 2009 Jun 11 (pp. 627-631). IEEE.

[30] Mandal D, Sharma D, Schamel H. Electron hole instability as a primordial step towards sustained intermittent turbulence in linearly subcritical plasmas. New Journal of Physics. 2018 Jul 4;20(7):073004.

[31] Barral S, Makowski K, Peradzyński Z, Dudeck M. Transit-time instability in Hall thrusters. Physics of Plasmas. 2005; 12:073504. Doi.org/ 10.1063/1.1947796

[32] Bello-Benítez E, Ahedo E. Axial-azimuthal, high-frequency modes from global linear-stability model of a Hall thruster. Plasma Sources Science and Technology. 2021 Jan;**20**

[33] T. Lafleur, S. D. Baalrud and P. Chabert, Theory for the anomalous electron transport in Hall Effect thrusters. II. Kinetic model, Phys. Plasmas 23,053503 (2016).

[34] Fan H, Li H, Ding Y, Wei L, Yu D. Effects of the peak magnetic field position on Hall thruster discharge characteristics. Advances in Space Research. 2020 Oct 15;**66**(8):2024-2034

[35] Sekine H, Koizumi H, Komurasaki K. Electrostatic ion acceleration in an inductive radio-frequency plasma thruster. Physics of Plasmas. 2020 Oct 22;**27**(10):103513

[36] Puerta J, Martin P, Maass F, Puerta JB, Brito J. Generalized non-ideal treatment and growth rates analysis of drift waves instabilities in a collisions-free magnetized dusty plasma. Physics of Plasmas. 2021 Feb 24;28(2):023701.

[37] Mikellides IG, Ortega AL. Growth of the modified two-stream instability in the plume of a magnetically shielded Hall thruster. Physics of Plasmas. 2020 Oct 5;**27**(10):100701

[38] Tomilin DA, Khmelevskoi IA. Influence of kinetic effects on long wavelength gradient-drift instability in high-frequency range in Hall thruster. Physics of Plasmas. 2020 Oct 1;**27**(10): 102103

[39] Marcovati A, Ito T, Cappelli MA. The dynamics of coherent modes of gradient drift instabilities in a small magnetron discharge plasma. Journal of Applied Physics. 2020 Jun 14;**127**(22): 223301

[40] Litvak AA, Fisch NJ. Resistive instabilities in Hall current plasma discharge. Physics of Plasmas. 2001 Feb; **8**(2):648-651

[41] Fernandez E, Scharfe MK, Thomas CA, Gascon N, Cappelli MA. Growth of resistive instabilities in E× B plasma discharge simulations. Physics of Plasmas. 2008 Jan 8;15(1):012102.

[42] Marusov NA, Sorokina EA, Lakhin VP, Ilgisonis VI, Smolyakov AI. Gradient-drift instability applied to Hall thrusters. Plasma Sources Science and Technology. 2019 Jan 11;28(1):015002.

[43] Ducrocq A, Adam JC, Héron A, Laval G. High-frequency electron drift instability in the cross-field configuration of Hall thrusters. Physics of Plasmas. 2006 Oct 20;**13**(10): 102111

[44] Litvak AA, Fisch NJ. Rayleigh instability in Hall thrusters. Physics of Plasmas. 2004 Apr 26;**11**(4):1379-1383

[45] Kapulkin A, Guelman MM. Low-frequency instability in near-anode region of Hall thruster. IEEE transactions on plasma science. 2008 Nov 17;**36**(5):2082-2087

[46] Choueiri EY. Plasma oscillations in Hall thrusters. Physics of Plasmas. 2001; **8**:1411-1426

[47] Esipchuk YB, Morozov AI, Tilinin GN, Trofimov AV. Plasma oscillations in closed-drift accelerators with an extended acceleration zone Sov. Phys.–Tech. Phys. 1974;**18**:928-932

[48] Parker JB, Raitses Y, Fisch NJ. Transition in electron transport in a cylindrical Hall thruster. Applied Physics Letters. 2010 Aug 30;97(9): 091501.

[49] Liqiu W, Ke H, Chunsheng W, Hong L, ChaoHai Z, Daren Y. Study on breathing mode oscillation suppression of self-excited Hall thrusters. Journal of Vacuum Science & Technology A: Vacuum, Surfaces, and Films. 2012 Nov 17;30(6):061304.

[50] Abramkov V V, Izmailov A A and Shishkin G G 1989 Influence of external circuit on characteristics of accelerator with closed electron drift and extended acceleration zone Proc. 7th All-Union Conference on Plasma Accelerators and Ion Injectors (Kharkov, 26–28 September, 1989) pp 72–3 (in Russian)

[51] Vakhnjuk S P, Kapulkin A M and Prisnjakov V F 1990 Stabilization of plasma instabilities in accelerators with closed electron drift by boundary system of feedback pp 78–86 in [24]

[52] Morozov AI, Nevrovskii VA, Smirnov VA. Effect of a feedback system on the plasma flux in an accelerator with closed electron drift. Sov. Phys.-Tech. Phys.(Engl. Transl.), v. 18, no. 3, pp. 344-347. 1973 Sep 1.

[53] Morozov A I 1973 The study of plasma systems with closed electron drift and distributed electric field pp 75–84 in [16]

[54] Kim V 1982 Main physical features of operational processes in modern

accelerators with closed electron drift and extended acceleration zone Proc. 5th All-Union Conf. on Plasma

[55] Bugrova A I and Kim V 1984 Modern state of physical studies in accelerators with closed electron drift and extended acceleration zone pp 107–28 in

[56] V. P. Lakhin, V. I. Ilgisonis, A. I. Smolyakov, E. A. Sorokina and N. A. Marusov, Effects of finite electron temperature on gradient drift instabilities in partially magnetized plasmas, Physics of Plasmas, 25(1) (2018), 012106.

[57] Romadanov I, Smolyakov A, Raitses Y, Kaganovich I, Tian T, Ryzhkov S. Structure of nonlocal gradient-drift instabilities in Hall E×B discharges. Physics of Plasmas. 2016; **23**(12):122111

[58] O. Koshkarov, A. I. Smolyakov, A. Kapulkin, Y. Raitses and I. Kaganovich, Nonlinear structures of lower-hybrid waves driven by the ion beam, Physics of Plasmas, 25(6) (2018), 061209.

[59] A.I. Smolyakov, O. Chapurin, W. Frias, O. Koshkarov, I. Romadanov, T. Tang, M. Umansky, Y. Raitses, I.D. Kaganovich and V.P. Lakhin, Fluid theory and simulations of instabilities, turbulent transport and coherent structures in partially-magnetized plasmas of discharges, Plasma Physics and Controlled Fusion, 59(1) (2016), 014041.

[60] Malik HK, Singh S. Conditions and growth rate of Rayleigh instability in a Hall thruster under the effect of ion temperature. Physical Review E. 2011 Mar 15;83(3):036406.

[61] Singh S, Malik HK. Role of ionization and electron drift velocity profile to Rayleigh instability in a Hall thruster plasma. Journal of Applied Physics. 2012 Jul 1;112(1):013307.

[62] Singh S, Malik H K, Nishida Y. High frequency electromagnetic resistive instability in a Hall thruster under the effect of ionization. Physics of Plasmas.2013; 20: 102109 (1-7).

[63] Singh S, Malik HK. Growth of low frequency electrostatic and electromagnetic instabilities in a Hall thruster. IEEE Transactions on Plasma Science. 2011;**39**:1910-1918

[64] Singh S, Malik HK. Resistive instabilities in a Hall thruster under the presence of collisions and thermal motion of electrons. The Open Plasma Physics Journal. 2011;**4**:16-23

[65] Malik H K and Singh S. Resistive instability in a Hall plasma discharge under ionization effect. Physics of Plasmas.2013; 20: 052115 (1-8).

[66] Yadav P, Gupta DN, Avinash K. Relativistic electron-beam assisted growth of oscillating two-stream instability of a plasma wave. Physics of Plasmas. 2017 Jun 14;24(6): 062107.

[67] Aria AK, Malik HK. Studies on waves and instabilities in a plasma sheath formed on the outer surface of a space craft. Physics of Plasmas. 2008 Apr 11;15(4):043501.

[68] Becatti G, Goebel DM and Zuin M. Observation of rotating magnetohydrodynamic modes in the plume of a high-current hollow cathode. Journal of Applied Physics. 2021 Jan 21; 129(3):033304.

[69] Morozov AI. Focusing of Cold Quasineutral Beams in Electromagnetic Fields. Soviet Physics Doklady. 1966;**10**: 775

[70] Grimaud L, Mazouffre S. Conducting wall Hall thrusters in magnetic shielding and standard configurations. Journal of Applied Physics. 2017 Jul 21;122(3):033305.

[71] Morozov AI, Lebedev SV. Plasma optics. InReviews of Plasma Physics/ Voprosy Teorii Plazmy/Вопросы Теории Плазмы 1980 (pp. 301-460). Springer, Boston. MA.

[72] Morozov A I, Bugrova A I, Desyatskov A V, Ermakov Y A, Kozintseva M V, Lipatov A S, Pushkin A A, Khartchevnikov V K and Banov D V. ATON-Thruster Plasma Accelerator, Plasma Physics Reports, Vol. 23, No. 7, 1997, pp. 587–597 (translated from Fizika Plazmy, Vol. 23, No. 7, 1997, pp. 635–645).

[73] Hofer RR, Peterson PY, Gallimore AD, Jankovsky RS. A high specific impulse two-stage Hall thruster with plasma lens focusing. IEPC-01-036, 27th International Electric Propulsion Conference, Pasadena. CA.

[74] Hofer RR, Jorns B A, Polk J E, Mikellides I G and Snyder JS, Wear test of a magnetically shielded Hall thruster at 3000 seconds specific impuls,IEPC-2013-033,(2013).

[75] W. Huang, Ph.D. thesis, Study of Hall Thruster Discharge Channel Wall Erosion via Optical Diagnostics, The University of Michigan (2011).

[76] Liu H, Niu X and Yu DR. Numerical study of azimuthal sheath structure and asymmetric anomalous erosion in a stationary plasma thruster. Journal of Plasma Physics. 2019 Apr;85(2).

[77] Choueiri EY. Fundamental difference between the two Hall thruster variants. Physics of Plasmas. 2001 Nov;**8**(11):5025-5033

[78] Hong L, Zhongxi N, Daren Y. Hall thruster with grooved walls. Journal of Applied Physics. 2013 Feb;**28**:113(8)

[79] Ding Y, Peng W, Sun H, Xu Y, Wei L, Li H, Zeng M, Wang F and Yu D. Effect of oblique channel on discharge characteristics of 200-W Hall thruster. Physics of Plasmas. 2017 Feb 14;24(2): 023507.

[80] Olano A, Tang H, Ren J, Zhang G, Li J. Modular Design of A Radial Scalled Hall Thruster for Different Magnetic Configurations. In 2019 IEEE Pulsed Power & Plasma Science (PPPS) 2019 Jun 23 (pp. 1-4). IEEE.

[81] Andreussi T, Giannetti V, Leporini A, Saravia MM and Andrenucci M. Influence of the magnetic field configuration on the plasma flow in Hall thrusters. Plasma Physics and Controlled Fusion. 2017 Oct 27;60(1):014015.

[82] Garrigues L, Fubiani G, Boeuf JP. Appropriate use of the particle-in-cell method in low temperature plasmas: Application to the simulation of negative ion extraction. Journal of Applied Physics. 2016 Dec 7;**120**(21): 213303

[83] Esipchuk YV and Tilinin GN. Drift instability in a Hall-current plasma accelerator. Sov. Phys.-Tech. Phys. (Engl. Transl.);(United States). 1976 Apr 1;21(4).

[84] Chable S and Rogier F. Numerical investigation and modeling of stationary plasma thruster low frequency oscillations. Physics of plasmas. 2005 Mar 10;12(3):033504.